FILE

INTERNAL DOCUMENT 148

I.O.S.

FLOW THROUGH THE STRAIT OF DOVER

D. PRANDLE

IOS INTERNAL DOCUMENT 148

NATURAL ENVIRONMENT RESEARCH COUNCIL

INSTITUTE OF OCEANOGRAPHIC SCIENCES

INSTITUTE OF OCEANOGRAPHIC SCIENCES

Wormley, Godalming,
Surrey, GU8 5UB.
(042-879-4141)

(Director: Dr. A. S. Laughton)

Bidston Observatory,
Birkenhead,
Merseyside, L43 7RA.
(051-652-2396)
(Assistant Director: Dr. D. E. Cartwright)

Crossway,
Taunton,
Somerset, TA1 2DW.
(0823-86211)
(Assistant Director: M.J. Tucker)

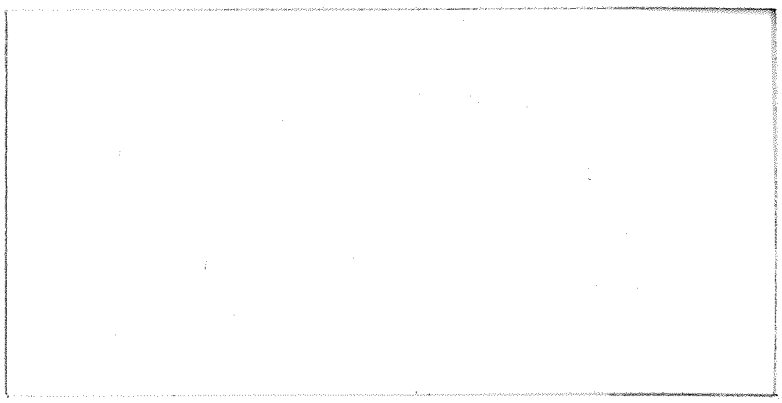

FLOW THROUGH THE STRAIT OF DOVER

D. PRANDLE

IOS INTERNAL DOCUMENT 148

ABSTRACT

This report has been compiled for the use of engineers involved in the design of bridge/tunnel crossings of the Dover Strait. Detailed information is provided on elevations, velocities and total flows associated both with the major tidal constituents and with meteorologically-induced surges. Data from various observational sources are collated and reviewed by reference to results obtained from a fine-grid (2.5 km) numerical model of the Dover Strait.

1. INTRODUCTION

Recently there has been renewed interest in the construction of a rail or road connection across the Dover Strait. Schemes under consideration include a proposed bridge and tunnel link with the bridge sections extending many kilometres into the Strait from both ends. Clearly schemes of this sort, which involve crossing the Strait as opposed to simply tunnelling underneath, require a detailed knowledge of local flow conditions. The present report aims to provide a substantial part of this information on flow conditions.

This region is one of the world's busiest navigation routes and as such has been studied extensively for many years. The shipping density and high currents combine to make off-shore measurements difficult and hazardous. Nevertheless, in recent years a number of oceanographic recordings have been made throughout this region. Inter-comparison of these recordings has proven their accuracy and reliability. Additionally, use is made here of a fine-grid (2.5 km) numerical model of the tidal propagation in the region to supplement observational data and to provide detailed spatial coverage.

A major part of this report deals with tidal propagation and information is provided for elevations, currents and net flows through the Strait. Meteorological influences, in particular the effect of wind-forcing, are also examined in some detail under the heading of "surges".

Wherever practical, essential information is listed here, otherwise references to basic sources are given. This report does not include information on (a) the wind-wave climate, (b) internal-waves or (c) sedimentation. The combination of high currents in relatively shallow depths promote rapid vertical mixing and probably preclude the propagation of interval-waves through this region.

2. OBSERVATIONAL DATA

The Dover Strait connects the southern North Sea with the English Channel (figure 1). These regions are characterised by strong tidal forcing and both are

subject to occasional high storm activity. The narrowest section is about 34 kms wide with depths of up to 50 m (figure 2).

2.1 Currents

Doodson (1930) analysed currents observed at the Varne Light-vessel (50°56'N, 1°17'E) over a two year period from 1922 to 1924. Recordings were taken 3 times daily at six depths, the tidal constituents derived from these recordings are discussed in section 4.

From 1920 to 1924, Carruthers (1925, 1927) used drift bottles to study the eastwards drift from the western end of the English Channel along the continental coast as far as the German Bight and beyond. These drift patterns established by Carruthers have been verified and quantified further by recent studies of the movement of Caesium released from the French nuclear plant at Cherbourg (Kautsky 1976). Carruthers (1928, 1935) also used a long series (1926 to 1932) of current meter recordings from the Varne to study the residual drift through the Dover Strait and, in particular, the relationship between this drift and the prevailing wind conditions.

Van Veen (1938) carried out an exhaustive series of current meter recordings throughout the Dover Strait region over the period 1934 to 1936. In total, he measured 300 profiles at 31 locations and in 1936 a further 392 profiles from a single location approximately 5 miles from Dover. From these measurements, he arrived at a parabolic representation for current profile in this region with $V(z) = V_S (z/D)^q$, where $V(z)$ the velocity at height z above the bed is related to the surface velocity V_S, D is the water depth and $q \simeq 0.02$. Van Veen derived tidal constants for 7 constituents and made estimates of average flood and ebb flow through the Strait and thereby the net residual flow.

In more recent times, flow measurements through the Dover Strait have been made by using cross-channel submarine telephone cables. The flow of a conducting material (sea water) across a magnetic field, i.e. the vertical component of the

earth's field, induces a potential difference proportional to the rate of flow. Bowden (1956) recorded this potential difference, using the telephone cable running from St. Margaret's Bay to Sangatte, over a 15 month period in 1953 and 1954. By comparing the voltage recordings with the tidal flow as predicted by Van Veen (1938) a calibration coefficient relating voltage to flow was deduced. Using this calibration coefficient, Bowden deduced flow magnitudes associated with eight tidal constituents. In addition, by examining the non-tidal component of the cable voltage he deduced a relationship between daily-mean values of flow, surface gradient and wind speed.

Cartwright (1961) and Cartwright and Crease (1963) also used cross-channel cable measurements to deduce the average sea-surface gradient between Dover and Dunkirk. Part of this study involved direct measurements of current profiles at six positions across the Strait over a five day period.

In 1973 the first deployment of automatic self-recording current meters was made in the Dover Strait. Recordings at three locations were obtained for periods of up to 49 days (Howarth and Loch 1977). The recordings formed part of an international oceanographic exercise in the southern North Sea referred to as JONSDAP '73. During this same exercise, simultaneous current measurements were made at four locations across the Strait over a period of 25 hours. These recordings are described by Prandle and Harrison (1975b). This paper also provides details of cable measurements recorded over a five-month period in 1973.

2.2 Elevations, salinity, temperature and meteorological data

A number of ports are located within the Dover Strait region (figure 1) and consequently shore-based tidal elevation data are plentiful. Table 1 shows the values of eight major constituents from ten ports. In addition, this table shows data from an off-shore tide gauge, TI, deployed for 46 days in 1973.

Long term monthly-mean values of temperature and salinity of the sea water (surface values) in this region are given by Smed (1970). Additional data are

available from Light-vessels and can be obtained from the Marine Information Advisory Service (M.I.A.S.) of I.O.S. Meteorological data are also available from these Light-vessels as well as from land-based recording stations. Wind data from Lympne, near Dover, have been used in studies of wind driven currents in this region (e.g. Bowden 1956). However, data recorded at sea are often more representative and Prandle (1978b) made use of data from the Dutch Light-vessel, Noord Hinder (51°39'N, 2°34'E). An alternative source for wind data may be obtained by using gradients of atmospheric pressure, by this means Schott (1970) calculated monthly mean winds for this region over the period 1950 to 1967.

3. NUMERICAL MODEL

The outer model of the southern North Sea extends northwards to latitude 53°20' and westwards to the Greenwich meridian (figure 1). The model is two-dimensional with velocities vertically averaged, the grid follows lines of latitude and longitude with spacings of 10' of longitude and $6\frac{2}{3}$' of latitude, i.e. approximate 12 km. In the Dover Strait region, between latitudes 50°46$\frac{2}{3}$' and 51°20', this grid is sub-divided by a factor of five resulting in a grid size approximately 2.5 km square. A comprehensive description of the numerical finite difference scheme employed is given by Prandle (1974). In the present application the use of a smaller grid size with an explicit finite difference scheme required the time-step to be reduced to 1 minute. The coupling between the fine and coarse grids was fully dynamic and hence the boundaries of the model were at the positions stated previously.

The dynamical equations used are :

$$\frac{\partial U}{\partial t} + U\frac{\partial U}{\partial x} + V\frac{\partial U}{\partial y} + g\frac{\partial Z}{\partial x} + g\frac{C_o U(U^2+V^2)^{1/2}}{(D+Z)^{4/3}} - \Omega V = 0 \qquad (1)$$

$$\frac{\partial V}{\partial t} + U\frac{\partial V}{\partial x} + V\frac{\partial V}{\partial y} + g\frac{\partial Z}{\partial y} + g\frac{C_o V(U^2+V^2)^{1/2}}{(D+Z)^{4/3}} + \Omega U = 0 \qquad (2)$$

$$\frac{\partial Z}{\partial t} + \frac{\partial}{\partial x}\left\{U(Z+D)\right\} + \frac{1}{\Delta x}\frac{\partial}{\partial y}\left\{V(Z+D)\Delta x\right\} = 0 \qquad (3)$$

where U, V are depth mean velocities along the x and y axes respectively,

x, y orthogonal axes positive to the east and to the north,

Δx grid length in the x direction,

Z elevation of the water surface above a horizontal datum,

D depth of the bed below the same datum,

ρ density of sea water,

C_o a friction coefficient, constant throughout the model,

Ω Coriolis parameter,

t time,

g gravitational acceleration.

For clarity the terms representing the influence of wind forcing and atmospheric pressure have been omitted from (1) and (2).

Model results cited in later sections were, in most instances, taken from a simulation of tides over a 15-day period, i.e. a complete spring-neap-spring cycle.

4. TIDES

4.1 Elevations

In the terminology used for tidal predictions, Dover is classified as a shallow-water port. This implies that non-linear interactions are important in this vicinity and, as a result, accurate tidal predictions by the "harmonic method" requires the use of 114 tidal constituents. The predominant constituent is M_2 with an amplitude of 2.23 m followed by S_2 with an amplitude of 0.71 m and N_2 with amplitude 0.41 m. Interest here will be restricted to these three major constituents together with the diurnal constituents O_1 and K_1 and the higher harmonics M_4, MS_4 and M_6. All the other constituents have amplitudes less than 0.10 m with the

exceptions of ν_2 (0.10 m), L_2 (0.14 m) and K_2 (0.20 m). The amplitude and phase of these eight constituents were previously shown in table 1 for 10 ports in the region and for one off-shore tide gauge, TI.

Prandle (1980) produced co-tidal charts for the southern North Sea and Dover Strait region for these eight constituents. The charts were constructed on the basis of all available tidal data (both tide gauge and current meter data) together with tidal distributions obtained from a numerical model of the region. For most purposes, these charts provide sufficient information on the propagation of tidal elevations through the Dover Strait. Similar co-tidal charts for the English Channel have been produced by Chabert D'Hieres and Le Provost (1978).

Figures 3(a) and 3(b) show a comparison of model and observed results for the amplitude and phase of the M_2 constituent, likewise figures 4(a) and 4(b) show similar comparisons for S_2. The results shown by Prandle (1980) should be used for data extraction, these latter figures are only included to indicate the accuracy of model results in this region. The results for M_2 show that the phase values in the model are in almost precise agreement with observation but that model amplitudes are about 10% larger than observations on the British coast and about 20% larger on the Continental coast. The comparisons for S_2 show that the phase in the model lags behind observed values by about 10° and the amplitude in the model is about 5% smaller than observed.

4.2 Currents

Tables 2(a) and 2(b) summarise the observed current data described in section 2.1. These data provide a good spatial representation of tidal currents in the Strait and, allowing for localised variability, there is good agreement between observations for all except the smallest constituents.

Component parts of figures 3 and 4 show model results for current ellipse properties for the constituents M_2 and S_2 respectively. Part (c) shows the major axis of the ellipse A, (d) the phase (or timing) of the maximum current Θ, (e) the

direction of the major axis α and (f) the eccentricity E. These model results show the spatial variability of the tidal components and may be compared with the distributions for A, θ and α shown by Sager (1968). While Sager's results are based on observed flow at the time of spring tide, there is close agreement between these results and the computed values shown in figures 3 and 4.

Observed values for α and E are indicated in figures 3(e), 3(f), 4(e) and 4(f) for ready comparison with model results. The eccentricity E denotes the ratio between minor and major axes of the current ellipse and a sign convention is appended to indicate direction of rotation (positive for anti-clockwise rotation). All four diagrams indicate close agreement between model results and observations.

Figures 5(a) and 5(b) show, for M_2 and S_2, a comparison of observed and model results for A and θ across a section of the channel between Dover (St. Margaret's Bay) and Sangatte. This section corresponds to the location of Cartwright's (1961) measurements and follows the line of the cross-channel telephone cables (figure 2). The observations from TQ, TO and TK lie a few kilometres north-east of this line and hence the phases at these positions should show some small lag relative to the other values. For M_2, the model values for A are about 18% larger than observations and the model phase leads by almost 30°. For S_2, the model values for A are in almost exact agreement with observations and the model phase leads by about 7°. Comparing these results with those for elevations described in the previous section (4.1), we note that for M_2, the larger amplitude in the model currents accompanies the larger range of elevation in the model. Whereas the 30° phase lead in the currents contrasts with the precise agreement in the elevation phases. For S_2, the exact agreement in current amplitudes differs only slightly from the 5% smaller amplitudes found in the model elevations while the 10° phase lag in model elevations is converted to a 7° phase lead in model currents.

In a more usual modelling simulation where the tidal energy propagates in a certain direction, the lack of agreement for M_2 could be corrected by increasing

friction in the direction from which the energy is propagating. This would normally decrease tidal amplitudes and delay tidal phases and some suitable compromise between the agreement for both elevations and currents could be achieved. However, in the Dover Strait tidal energy propagates from both the English Channel and the North Sea and the observed conditions may be seen as a vector addition of the two tidal systems. Adjustment of the model under these conditions is clearly more complex. In addition, it is likely that tidal conditions in the Strait might be sensitive to small relative changes in boundary conditions specified along the open-boundaries of the southern North Sea model (figure 1).

This latter point may be readily understood by noting, from figure 3(d) that the current phase along the Strait changes by 30^{o} in as little as about 10 kms and hence only a slight modification to the spatial pattern is required to account for the discrepancy between model results and observations. An additional point of interest shown by both figures 3(d), 4(d), 5(a) and 5(b) is the large phase variation across the channel with a 'boundary' layer at each side showing phase leads of up to 60^{o} relative to the central section. Van Veen (1938) observed similar effects in the boundary regions. This 'early reversal' at the boundaries is commonly experienced in estuaries; it is attributed to bed-friction and in mid-channel a related phase difference is generally found between flow at the bed and at the surface. In the model, the phase of the current in this region is almost directly related to the bed friction term and hence reflects the current phase at the bed. The observed currents generally reflect depth-averaged conditions and no clear mention has been made of significant phase changes through depth in these observations. However, in view of the difficulties of measuring currents very close to the bed in this region, it is possible that a significant phase advance exists which could explain the difference between model and observed results.

The complexity of the tidal propagation can be seen from the relationship between flow and elevation. Thus comparing the elevation data for Dover shown

in Table 1 with the current data from Table 2(a), we find for the semi-diurnal constituents, that the phase of the elevation leads the current phase by about 30°. In an estuarine system we normally expect this phase difference to vary between 0° for a progressive wave and -90° for a standing wave. The present phase difference, $\Psi = 30^{\circ}$, indicates that there is a net propagation of tidal energy into the North Sea (i.e. $\cos\Psi > 0$) and the unusual phase relationship may be attributed to the vector addition noted earlier. (The complex results of such vector addition may be understood by adding two arbitrary wave components and then adjusting the ratio of current to elevation amplitude in one component). For the diurnal constituents the phase of the elevation leads the current by an angle in the range 90° to 270° indicating that the tidal energy propagates out of the North Sea (i.e. $\cos\Psi < 0$). This latter result is confirmed by the progression of elevation phases towards the Channel for both O_1 and K_1 shown by Prandle (1980).

Comparing the amplitude ratios of the various data sets in Tables 1 and 2(a) we find the ratios of $S_2 : M_2$ and $N_2 : M_2$ are almost identical between various current meters, the cable voltage and the elevation at Dover. Similarly the ratios of M_4, M_{S4} and M_6 to M_2 are similar for these various data sets although some variability arises due to the inaccuracy associated with the determination of these constituents. By contrast the ratios of $O_1 : M_2$ and $K_1 : M_2$ in the elevation data are approximately one-third of the corresponding ratios in the current meter and cable data sets. The smaller relative values of elevation for these latter constituents may be attributed to the close proximity of amphidromic points as shown by Prandle (1980).

Determination of the longer period tidal constituents for the flow data is difficult due to their small amplitudes and the need for a long recording period to eliminate meteorological effects or other 'noise components' such as instrumental errors. From an analysis of 10 years of cable recordings, Alcock and Cartwright (1977) obtained a value for MS_f of 16 mV or about 1/50 of the value

for M_2. The value for MS_f at the same location in the model is about 2.6 cm s^{-1} or, again, about 1/50 of the value for M_2.

The cross-sectional area of the Dover-Sangatte line is approximately 1.22 x 10^6 m^2. By taking a vector mean of tidal constituents at TQ, TO and TK we calculate (a) for M_2, a velocity amplitude of 106 cm s^{-1} or a net flow amplitude of 1.29 x 10^6 m^3s^{-1} and (b) for S_2, a velocity of 36 cm s^{-1} with a net flow of 0.44 x 10^6 m^3s^{-1}. By taking a similar vector mean of Cartwright's (1961) data we obtain (a) for M_2, 113 cm s^{-1} or 1.38 x 10^6 m^3s^{-1} and (b) for S_2, 38 cm s^{-1} or 0.46 x 10^6 m^3s^{-1}. For the model, corresponding values are (a) for M_2, 130 cm s^{-1} or 1.43 x 10^6 m^3s^{-1} and (b) for S_2, 36 cm s^{-1} or 0.40 x 10^6 m^3s^{-1}.

5. SURGES

All non-tidal phenomena are here summarised under the heading of "surges", in general the concern is with meteorologically generated flows. The physics of surge generation in this region has been described by Heaps (1967), interest here will be restricted to flow and elevation data within the Dover Strait.

Table 3 shows pertinent elevation data for Dover taken from the Admiralty Tide Tables (ATT) and from a study of sea level maxima carried out by Graff (1981). The storm levels cited correspond to the highest estimates given by Graff. Table 4 shows related flow data for the Dover Strait. Values for the M_2 and S_2 tide were taken from the numerical model, Neap tide corresponds to $M_2 - S_2$ and Spring tide to $M_2 + S_2$. The additional values shown in this table were obtained by assuming the same proportional factors as shown for the elevation data in Table 3. Thus the ratio $HAT/_{MHWS}$ in Table 3 is assumed to apply between $HAT/_{Spring\ tide}$ in Table 4. From related studies carried out elsewhere it is expected that the estimates for flow data in Table 4 might be too large, interaction effects limit extreme flows to a greater degree than extreme elevations. As a check on these estimates we can examine data for the 1953 surge. Graff shows that this surge was the largest yet

recorded at Dover and corresponds to the 1 in 100 year return level. Prandle (1975a) showed that the flow through the Dover Strait for this surge reached a maximum of about 2.60×10^6 $m^3 s^{-1}$ whereas Table 4 gives a value of 2.78×10^6 $m^3 s^{-1}$ for the 1 in 100 year storm.

It is possible that the maximum elevation and maximum flow occurring in a particular storm do not correspond to the same level of probability. In addition, the geometry of the surrounding regions introduces some assymetry into the probability distribution of positive (towards the North Channel) and negative flows. Table 5 shows a relationship derived by Prandle (1978a) between wind direction and flow through the Strait for a wind speed of 15 knots. This Table represents an averaged response to a steady wind speed as calculated from modelling studies. While these results were shown (Prandle 1978a) to be in good agreement with similar results found by Bowden (1956), they should be used with due caution. Noting that the flow Q_W is proportional to wind speed squared, the wind speed corresponding to a particular return period can be estimated by scaling up the values in Table 5 to account for the difference between storm flows and maximum tidal flows as shown in Table 4. Thus the 1 in 250 year storm flow could be obtained when a steady wind speed of 43 knots blows in a northerly direction in combination with a spring tide. The equivalent wind velocities for the 1 in 50 and 1 in 100 year storms are 36 knots and 39 knots respectively.

In addition to the meteorologically-induced flow there is a more or less permanent residual flow towards the North Sea due both to the non-linearities associated with tidal flow and to the oceanic-scale flow across the continental shelf. The exact magnitude of this steady residual is difficult to estimate (Otto 1982), here it is convenient to adopt Prandle's (1978a) estimate of 123×10^3 $m^3 s^{-1}$.

The fine grid model (figure 1) indicates considerable variation in the cross-sectional distribution of residual flows. At either end and in the middle of the

Dover-Sangatte section the residual current is towards the North Sea but in the two intermediate zones the residual current is in the opposite direction. The residual flow is similarly variable, although for the Dover-Sangatte section it is always towards the North Sea with one small exception about 8 kms from Dover. Van Veen (1938) reported similar cross-sectional variations in residual flow.

Using the above estimate for residual flow together with the relationships between wind speed and flow shown in Table 5 Prandle (1978b) estimated monthly-mean residual flows through the Dover Strait for the years 1949-1972. Table 6 shows part of these results listing the annual flows for the years 1961 to 1972 and the mean-monthly values averaged over the 24 year period. The monthly variations agree well with similar estimates made by Carruthers (1935).

References

ALCOCK, G.A. and CARTWRIGHT, D.E. 1978. An analysis of 10 years' voltage records from the Dover-Sangatte cable. pp.341-365 in, A voyage of discovery, George Deacon 70th Anniversary Volume, (ed. M. Angel). Oxford: Pergamon. 696 pp.

BOWDEN, K.F. 1956. The flow of water through the Straits of Dover related to wind and differences in sea level. Philosophical Transactions of the Royal Society of London, A, 248, 517-551.

CARRUTHERS, J.N. 1925. The water movements in the Southern North Sea. Part 1. The Surface Drift. Fishery Investigations, Ser.2, 8(2), 119 pp.

1927. Investigations upon the water movements in the English Channel. Summer, 1924. Journal of the Marine Biological Association of the U.K.

1928. The flow of water through the Straits of Dover as gauged by continuous current meter observations at the Varne Lightvessel. Part 1. Fishery Investigations, Ser.2, 11(1), 109 pp.

1935. The flow of water through the Straits of Dover. Fishery Investigations, Ser.2, 14(4), 67 pp.

CARTWRIGHT, D.E. 1961. A study of currents in the Straits of Dover. Journal of the Institute of Navigation, 14(2), 130-151.

CARTWRIGHT, D.E. and CREASE, J. 1963. A comparison of the geodetic reference levels of England and France by means of the sea surface. Proceedings of the Royal Society of London, A, 273, 558-580.

CHABERT D'HIERES, M.G. and LE PROVOST, C. 1978. Atlas des compasantes harmoniques de la maree dans la Manche. Annales Hydrographiques, Ser.6, 5-36.

DOODSON, A.T. 1930. Current observations at Horn's Rev., Varne and Smith's Knoll in the years 1922 and 1923. Journal du Conseil, 5, 22-32.

GRAFF, J. 1981. An investigation of the frequency distributions of annual sea level maxima at ports around Great Britain. Estuarine, Coastal and Shelf Science, 12, 389-449.

HEAPS, N.S. 1967. Storm Surges. Oceanography & Marine Biology, an annual review, 5, 11-47.

HOWARTH, M.J. and LOCH, S.G. 1977. Moored current meter records, southern North Sea; 6 Sept. - 28 Oct. 1973; IOS Bidston Moorings 37-43. Institute of Oceanographic Sciences, Data Report No.14, 102 pp. (Unpublished manuscript).

KAUTSKY, H. 1976. The Caesium 137 content of the North Sea during the years 1969 to 1975. Deutsche Hydrographische Zeitschrift, 29(6), 217-221.

OTTO, L. (in preparation) (author CH.8. Straits of Dover) Flushing times of the North Sea. International Council for the Exploration of the Sea.

PRANDLE, D. 1974. A numerical model of the southern North Sea and River Thames. Institute of Oceanographic Sciences, Report No.4, 24 pp. (Unpublished manuscript).

PRANDLE, D. 1975a. Storm surges in the southern North Sea and River Thames. Proceedings of the Royal Society of London, A, 344, 509-539.

PRANDLE, D. and HARRISON, A.J. 1975b. Relating the potential difference measured on a submarine cable to the flow of water through the Strait of Dover. Deutsche Hydrographische Zeitschrift, 28, 207-226.

PRANDLE, D. 1978a. Residual flows and elevations in the southern North Sea. Proceedings of the Royal Society of London, A, 359, 189-228.

PRANDLE, D. 1978b. Monthly mean residual flows through the Dover Strait, 1949-1972. Journal of the Marine Biological Association of the U.K., 58, 965-973.

PRANDLE, D. 1980. Co-tidal charts for the southern North Sea. Deutsche Hydrographische Zeitschrift, 33, 68-81.

SAGER, G. 1968. Tidal streams in the Straits of Dover. Seeverkehr 11, 458-460.

SCHOTT, F. 1970. Monthly mean winds over the sea areas around Britain during 1950-1967. Charlottelund Slot, Denmark : International Council for the Exploration of the Sea, Hydrographic Service. 17 pp.

SMED, J. 1970. Monthly means of surface temperature and salinity for areas of the North Sea and the north-eastern North Atlantic. Charlottelund Slot, Denmark. International Council for the Exploration of the Sea, Hydrographic Service.

VAN VEEN, J. 1938. Water movements in the Straits of Dover. Journal du Conseil, 14(2), 130-151.

List of figures

1. Schematic representation of the southern North Sea and Dover Strait.

2. Dover Strait : depth contours, observational locations and submarine cable alignment.

3. Propagation of the M_2 tide through the Dover Strait.

   Contours indicate model results and point measurements indicate observed values (units cgs)

   (a) elevation amplitude;

   (b) elevation phase (relative to the lunar transit at Greenwich);

   (c) amplitude of the major axis of the current ellipse, A ;

   (d) phase of the maximum current, θ ;

   (e) direction of the major axis, α , measured clockwise from north;

   (f) eccentricity, E.

   E is defined as the ratio of the minor axis : major axis, in addition E is positive for an anticlockwise rotating ellipse and negative for clockwise rotation.

4. Propagation of the S_2 tide through the Dover Strait.
   Legend as for Figure 3.

5. Comparison of observed and model results for currents across the Dover-Sangatte section.

   A - major axis; θ current phase.

   ———— model, - - - - - Cartwright's (1961) measurements;

   ● TO, TQ and TK.

List of Tables

1. Tidal Elevations.

   Amplitude (cm) and phase (g) of major tidal constituents.

   Sources : ICOT '63 Institute of Coastal Oceanography and Tides ('63 indicates year of observation).

   ATT Admiralty Tide Tables.

   IHB International Hydrographic Bureau.

   EPSHOM Establissement Principal du Service Hydrographique et Oceanographique de la Marine.

   Data length; Y - year, D - day.

2. (a) Current Observations.

   Amplitude of the major axis of the ellipse (cm s^{-1}).
   Phase of the maximum current.
   Cable data in mV.

   Data length; Y - year, D - day.
   Data locations shown in figure 2.

(b) Additional current ellipse data.

Direction of the major axis measured clockwise from north.
Ellipticity, negative indicates clockwise rotation.

3. Elevation data for Dover.

Sources : Tidal data - ATT, storm levels - Graff (1981).
Data in metres above O.D.N., chart datum = -3.67 O.D.N.

4. Average velocities and total flow through the Dover Strait (Dover-Sangatte section).

5. Directional response to wind forcing (Prandle 1978a).

QW is proportional to the square of the wind speed and positive for flows into the North Sea.

6. Estimates of annual residual flows (Q_A) and mean monthly values (Q_M), (Prandle 1978b).

LOCATION	LAT N	LONG E	SOURCE	DATA LENGTH	O_1	K_1	N_2	M_2	S_2	M_4	MS_4	M_6
Ramsgate	51°20	1°25	ICOT '63	1 Y	9,182°	7,12°	35,318°	186,339°	56,30°	13,241°	8,287°	4,125°
Deal	51°13	1°25	ATT		7,175°	6,20°		207,336°	63,27°			
Dover	51°07	1°19	IOS '75	1 Y	6,172°	6,46°	41,309°	223,332°	71,23°	27,220°	17,273°	7,104°
Folkestone	51°05	1°12	ATT		2,241°	5,55°		245,332°	79,32°			
Hastings	50°51	0°35	IHB	30 D	2,223°	8,95°	44,294°	247,323°	89,17°	22,228°	15,283°	4,173°
Ostend	51°14	2°55	ICOT '43	1 Y	8,174°	4,346°	29,339°	176,5°	52,58°	9,337°	7,37°	7,300°
Nieuport	51°09	2°43	ICOT '43	1 Y	10,174°	5,354°	32,336°	186,0°	54,52°	13,310°	8,8°	5,268°
Dunkirk	51°03	2°22	ICOT '58	1 Y	7,157°	4,9°	36,330°	211,353°	63,46°	15,279°	9,337°	3,214°
Calais	50°58	1°51	ICOT '41	1 Y	4,147°	1,62°	43,320°	238,341°	76,33°	22,241°	15,295°	5,125°
Boulogne	50°44	1°35	EPSHOM	1 Y	4,77°	18,135°	52,310°	293,331°	96,21°	33,222°	22,275°	6,90°
TI	51°09	1°47	ICOT '73	46 D	10,162°	6,26°	35,324	206,345°	66,35°	17,253°	14,297°	3,157°

Table 1. Tidal Elevations.

Amplitude (cm) and phase (relative to the moon's transit at Greenwich) of major tidal constituents.

Sources: ICOT '63; Institute of Coastal Oceanography and Tides ('63 indicates year of observation).

ATT : Admiralty tide tables.

IHB : International Hydrographic Bureau.

EPSHOM : Etablissement Principal du Service Hydrographique et Oceanographique de la Marine.

Data length : Y - year, D - day.

SOURCE	LAT N	LONG E	DATA LENGTH	O_1	K_1	N_2	M_2	S_2	M_4	MS_4	M_6
Doodson (1930) 1922	50°56	1°17	1Y	9,217°	11,84°		72,0°	23,56°		5,72°	
1923			1Y	6,204°	6,21°		78,348°	26,27°		1,185°	
Van Veen (1938)	51°04	1°25	16D	13,31°	10,177°		109,7°	26,60°	10,286°		
TK J'73	51°05	1°47	46D	11,46°	11,193°	19,357°	105,5°	36,54°	13,276°	11,319°	2,179°
TQ J'73	51°09	1°31	44D	12,52°	12,181°	22,0°	106,8°	33,53°	13,286°	8,176°	3,204°
TO J'73	51°04	1°35	32D	11,56°	11,201°	20,353°	108,11°	38,57°	12,274°	9,315°	2,168°
C Cartwright 1961	51°07	1°26	2D	8,335°	5,199°	16,333°	103,354°	35,45°	12,274°	8,323°	5,220°
B "	51°05	1°30	2D	11,4°	8,228°	20,353°	121,14°	41,65°	22,293°	14,342°	1,110°
A "	51°04	1°33	2D	14,12°	8,236°	18,352°	110,13°	37,64°	22,268°	14,317°	2,358°
A` "	51°02	1°35	2D	13,9°	8,233°	17,349°	107,10°	36,61°	19,284°	12,333°	1,290°
B` "	51°0	1°38	2D	12,345°	7,209°	20,341°	124,2°	42,53°	20,260°	12,309°	1,149°
C` "	50°59	1°41	2D	9,0°	5,224°	18,331°	119,352°	38,43°	16,257°	10,306°	6,204°
Cable Data, Prandle & Harrison (1975b)			128D	81,41°	60,199°	132,343°	720,1°	259,52°	80,285°	58,333°	12,190°

Table 2(a) Current Observations.

Amplitude of the major axis of the current ellipse in cm s^{-1}.

Phase of the maximum current (for velocities approximately NE except as stated in table (b)).

Cable data in mV.

Data length : Y - year, D - day.

Data locations shown in figure 2.

		O_1	K_1	N_2	M_2	S_2	M_4	MS_4	M_6
Doodson	1922	54°,-.02	41°,-.01		33°,-.16	36°,-.20		272°,-.09	
	1923	53°,-.02	53°,-.13		34°,-.15	33°,-.14		23°,-.08	
TK		54°,-.00	57°,-.02	53°,.04	54°,.06	55°,.07	50°,.10	50°,.11	45°,.18
TQ		47°,-.05	40°,.02	42°,.02	43°,-.08	42°,-.09	45°,.06	329°,-.38	38°,-.18
TO		50°,.07	57°,.03	51°,-.04	51°,.02	51°,.01	56°,.20	55°,.23	61°,.53

Table 2(b) Additional current ellipse data.

Direction of major axis measured clockwise from north.

Ellipticity,- ve clockwise rotation.

Mean Low Water Springs	(MLWS)	- 2.87
Mean Low Water Neaps	(MLWN)	- 1.67
Mean Water Level	(MWL)	.03
Mean High Water Neaps	(MHWN)	1.63
Mean High Water Springs	(MHWS)	3.03
Highest Astronomical Tide	(HAT)	3.63
1 in 50 year Storm Level		4.37
1 in 100 year Storm Level		4.58
1 in 250 year Storm Level		4.89

Table 3 Elevation data for Dover.

Sources, tidal data ATT, storm levels, Graff (1981).
Data in metres above ODN; chart datum = -3.67 ODN.

	Average velocities ($m\ s^{-1}$)	Total flow ($10^6 m^3 s^{-1}$)
M_2 tide	1.30	1.43
S_2 tide	.36	0.40
Neap tide	0.94	1.03
Spring tide	1.66	1.83
HAT	1.99	2.20
1 in 50 year Storm	2.40	2.65
1 in 100 year Storm	2.52	2.78
1 in 250 year Storm	2.71	2.98

Table 4 Average velocities and total flow through the Dover Strait (Dover-Sangatte section).

Wind 15 knots from	flow, Q_W ($10^3 m^3 s^{-1}$)
N	-116
NE	-118
E	- 59
SE	55
S	142
SW	139
W	49
NW	- 53

Table 5

Directional response to wind forcing (Prandle 1978a).

Q_W is proportional to the square of the wind speed and positive for flows into the North Sea.

	Q_A ($10^3 m^3 s^{-1}$)		Q_M ($10^3 m^3 s^{-1}$)
1961	177	Jan.	170
1962	164	Feb.	135
1963	153	Mar.	127
1964	139	April	120
1965	162	May	130
1966	161	June	137
1967	182	July	157
1968	145	Aug.	168
1969	135	Sept.	161
1970	154	Oct.	170
1971	138	Nov.	182
1972	161	Dec.	201
		(Mean	155)

Table 6 Estimates of annual residual flow (Q_A) and mean monthly values (Q_M) (Prandle 1978b).

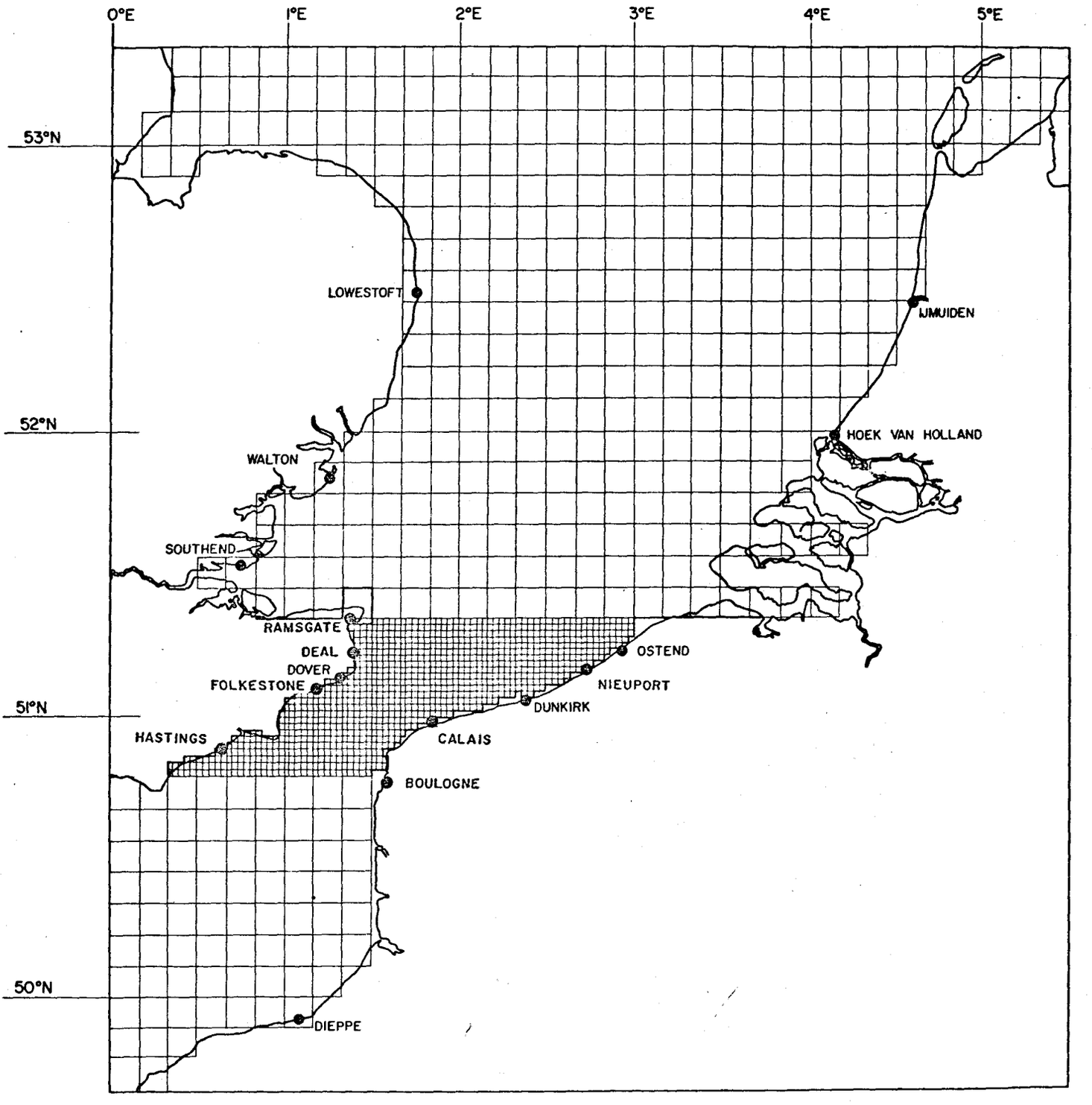

FIGURE 1 : SCHEMATIC REPRESENTATION OF THE SOUTHERN NORTH SEA.

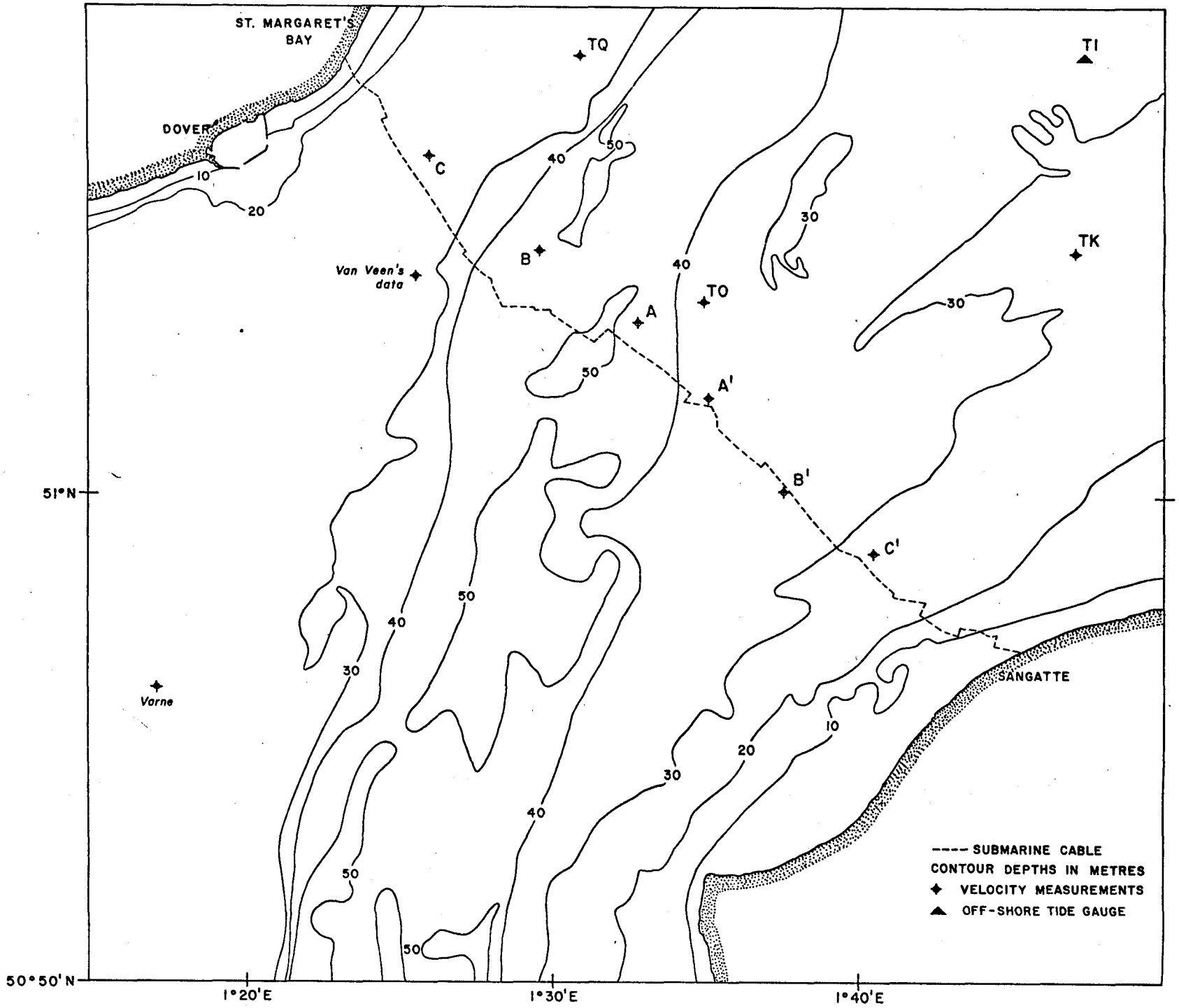

Figure 2 DOVER STRAIT

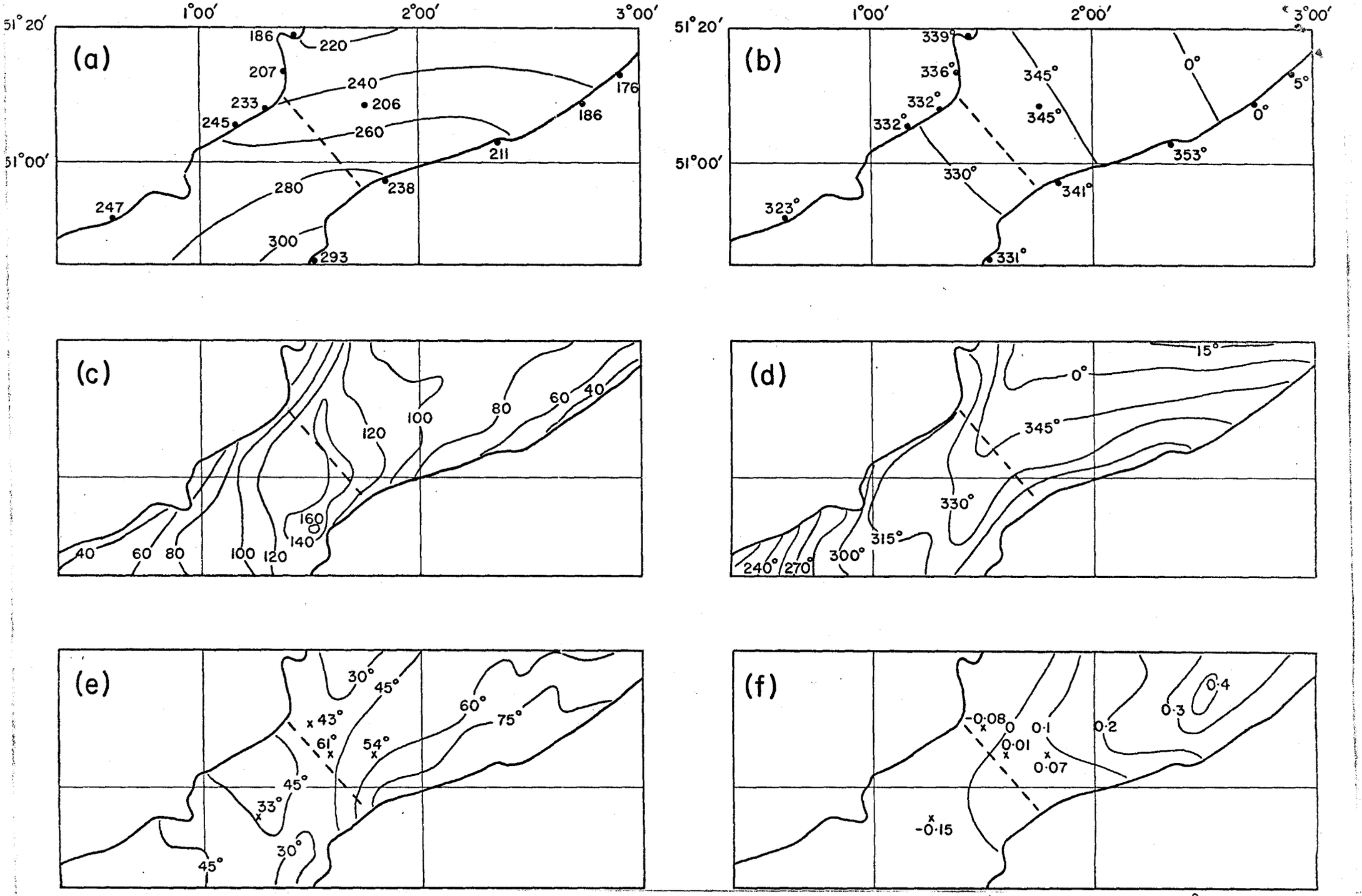

3. Propagation of the M_2 tide through the Dover Strait.

Contours indicate model results and point measurements indicate observed values (units cgs)

(a) elevation amplitude;

(b) elevation phase (relative to the lunar transit at Greenwich);

(c) amplitude of the major axis of the current ellipse, A;

(d) phase of the maximum current, θ;

(e) direction of the major axis, α, measured clockwise from N

(f) eccentricity, E.

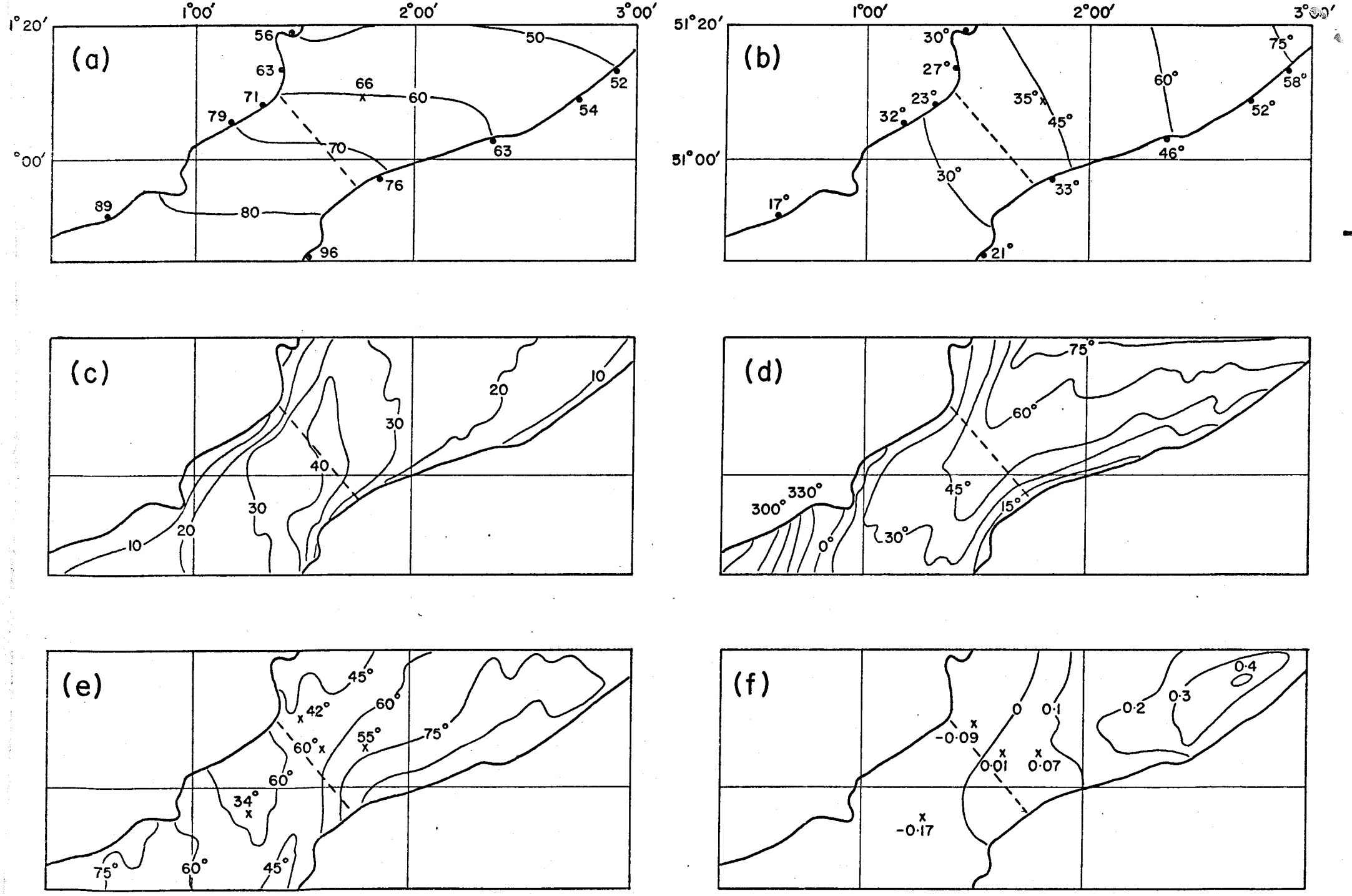

4. Propagation of the S_2 tide through the Dover Strait.
Legend as for Figure 3.

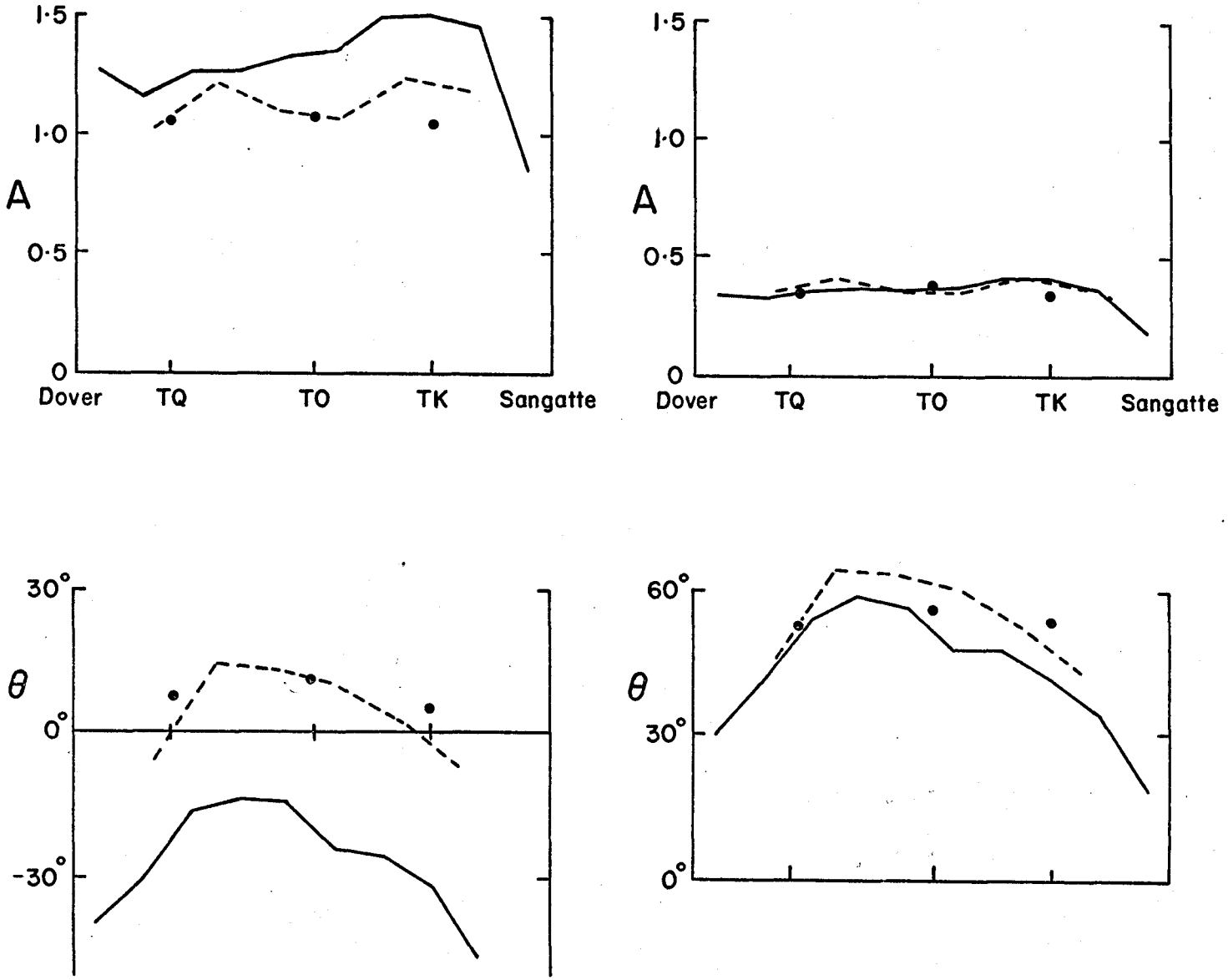

(a) M_2 (b) S_2

5. Comparison of observed and model results for currents across the Dover-Sangatte section.

A - major axis; θ current phase.

———— model, - - - - - Cartwright's (1961) measurements;

● TO, TQ and TK.